Automatic salt-body classification using deep-convolutional neural network

Conference Paper · August 2018

DOI: 10.1190/segam2018-2997304.1

Automatic salt-body classification using a deep convolutional neural network

Yunzhi Shi, Xinming Wu and Sergey Fomel, The University of Texas at Austin*

SUMMARY

We apply deep learning techniques to the problem of the salt body detection in seismic images. We consider salt body classification as an image segmentation problem, and propose to design a multi-layer convolutional neural network, feed in training data to train this network, and test the model using blind test data. Our results indicate that the proposed network architecture and workflow are capable of capturing subtle salt features automatically without the need for manual input. Trained with a limited amount of inline sections, the model can generalize to the blind test data and be efficiently applied to a whole 3D volume of seismic data.

INTRODUCTION

Salt boundary interpretation is important for understanding of salt tectonics and velocity-model building for seismic migration (Hudec et al., 2011). Interpreting salt boundaries often involves computing a salt attribute image and picking salt boundaries. Although automatic methods have been proposed for computing salt attributes and extracting salt boundaries (Ramirez et al., 2016; Wu et al., 2017); it remains in practice a human-intensive and time-consuming task.

In seismic interpretation and subsurface modeling, extracting geological structure features such as faults, unconformities, horizons and salt boundaries from 3-D seismic data are critical. Conventional methods derive seismic attributes from geological, physical and geometrical principles. Specifically, for automatic salt boundary interpretation, it requires computing salt attributes such as discontinuities (Asjad and Mohamed, 2015), textures (Wang et al., 2015), reflection dip or normal vector fields (Haukås et al., 2013), and salt likelihoods (Wu, 2016).

The hand-engineered attributes are designed with expertise knowledge; however, these attributes may not yet fully describe the complex noise-contaminated real-world seismic data (Marfurt and Alves, 2014). The recently developed machine learning techniques enable computers to perform repetitive tasks, and unravel the relationships that underlay repetitive patterns (Zhao, 2017). Recent works (Zhang et al., 2014; Frogner et al., 2015; Dahlke et al., 2016) demonstrate a new approach that applies a deep learning statistical model to transform raw-input seismic data directly to the final mapping of geological features. Deep neural networks (DNN) are built on the premise that they can replicate any nonlinear operator. Compared to traditional machine learning algorithms, DNNs have the advantage that it extracts useful features automatically. Recently, Ross and Cole (2017) review popular facies classification methods based on machine learning algorithms. Huang et al. (2017) show that CNN provides improved results over traditional methods such as support vector machines (SVMs) and logistic regression for identifying geologic faults in 3D seismic volumes. These experiments show encouraging accuracy in a variety of seismic processing and interpretation tasks. Araya-Polo et al. (2017) use prestack seismic data, without processing the data to seismic image, to identify faults. Waldeland and Solberg (2017) train a CNN to perform pixel-by-pixel salt body classification.

Previous researchers (Lomask et al., 2007; Ramirez et al., 2016) discuss salt boundary extraction as a global image segmentation problem. Considering it as an image segmentation address an important drawback of some deep learning approaches which only adopt networks designed for object categorization for pixel-wise labelling (Brostow et al., 2008; Sturgess et al., 2009; Grangier et al., 2009). It is necessary to build a mechanism to map deep layer feature back to the same dimension of the input images; those approaches resort to ad hoc methods to upsample features, e.g. by element replication.

We propose to adopt an alternative network architecture, inspired by Segnet (Badrinarayanan et al., 2017) and U-Net (Ronneberger et al., 2015), that overcomes the problem by learning to map encoder outputs to final classification labels of image dimension. This architecture is composed of a stack of encoders followed by a corresponding decoder stack which feeds into a softmax classification layer. Both encoder and decoder are fully convolutional layers. In order to test the proposed architecture, we generate salt body labels interactively with the aid of automatic tools (Wu et al., 2017). We first train the network on the selected 2D slices, then validate the model by predicting salt body location on other unseen slices.

MODEL ARCHITECTURE

We formulate salt body classification as a semantic image segmentation problem with binary classes: the algorithm assigns a salt label to each image pixel based on the shape of the seismic image. While multiple seismic attributes can aid the salt body detection, for simplicity, we only use seismic amplitude as the input in our automated method.

The framework of the proposed method is a convolutional encoder-decoder network. It is designed to be an efficient architecture for pixel-wise semantic segmentation. It is primarily borrowed from Segnet (Badrinarayanan et al., 2017), an architecture applied to road scene understanding applications which require the ability to extract the spatial relationship between object shape and the corresponding classes. The network has the ability to delineate objects based on their shape despite their small size. Compared to previous network architectures, this encoder-decoder architecture can be trained end-to-end in order to jointly optimize all the model parameters in the network.

The proposed network architecture is illustrated in Figure 1. The key component of our proposed network is the decoder network which consists of a hierarchy of decoders correspond-

10.1190/segam2018-2997304.1

ing to each encoder. The original Segnet reuses the max-pooling indices received from the encoders to perform non-linear upsampling of decoder feature maps, but this type of upsampling is prone to checkerboard artifacts (Odena et al., 2016). While these artifacts are acceptable in normal scale natural images, the issue becomes significant in seismic images which contain small scale features such as reflection signals, faults and tiny discontinuities. To overcome this issue, we adopt the resize-convolution proposed by Odena et al. (2016) in our implementation.

Each encoder in the encoder network performs convolution with a filter bank to produce a set of feature maps. These are then regularized by batch normalization (Ioffe and Szegedy, 2015). Element-wise rectified-linear unit ($\sigma(x) = \max\{0,x\}$) is applied as non-linear activation. Following that, we perform max-pooling and the resulting output is sub-sampled by a factor of 2. Max-pooling achieves translation invariance over small spatial shifts in the input image. The appropriate decoder in the decoder network upsamples its input feature maps by resizing-interpolation. This step produces sparse feature maps which are convolved with a trainable decoder filter bank to produce dense feature maps. Batch normalizations are also applied. The high dimensional feature representation at the output of the final decoder is fed to a trainable softmax classifier. The output of the classifier is a K channel image of classification probabilities, where K is the number of classes. In the case of salt detection, we define $K = 2$ where pixels are classified as inside/outside salt body.

TRAINING

We train and test the network using SEAM Phase 1 dataset (Fehler and Keliher, 2011). This dataset contains a 3D seismic volume which a salt body exists in the middle. We use the 2D single-channel seismic amplitude data as our input to the network. The challenge is to identify the salt body, from a noisy seismic image. The network can only learn from the subtle features such as high reflectivity and largely dipped boundary.

We selected 8 crossline 2D slices as training data. The training labels are manual annotations generated by optimal path picking method (Wu et al., 2017). Before each epoch, the training set is shuffled. Compared to the size of the model, this is a fairly small dataset; however, the bottleneck architecture ensures that essential relationship are captured.

The model weights, or parameters, are initialized using the technique described in He et al. (2015). We use the cross-entropy loss as the objective function, and adaptive momentum descent (Adam) as optimization algorithm (Kingma and Ba, 2014) to iteratively update the model weights.

After 200 epochs of training, the model achieves 98.77% global accuracy (the percentage of pixels correctly classified in the image). Figure 2 shows the training results of selected data samples. The salt likelihood is the probability output of the softmax classifier, and the predictions are assigned by max-likelihood class. Compared to the ground truth, the training accuracy is nearly as good as the human interpretation. How-

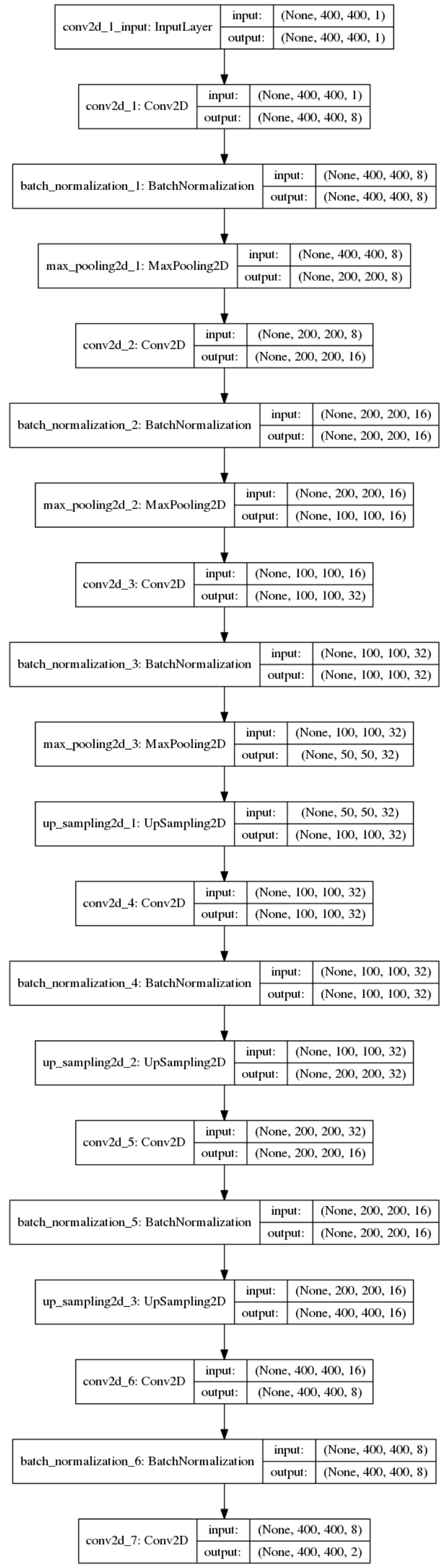

Figure 1: Architecture of the encoder-decoder network. The input and output shapes are listed in the format: `[samples_number, image_height, image_width, channels_number]`. All `samples_number`s are not fixed in the network since multiple data samples can run in parallel. Note that the initial input image has 1 channel (seismic amplitude) and the final output has 2 channels (binary classification). The intermediate channels represent multiple feature maps.

10.1190/segam2018-2997304.1

ever, this result is not suprising considering the large model size and small data size. To prove its effectiveness, the model needs to be validated by unseen samples not used in training.

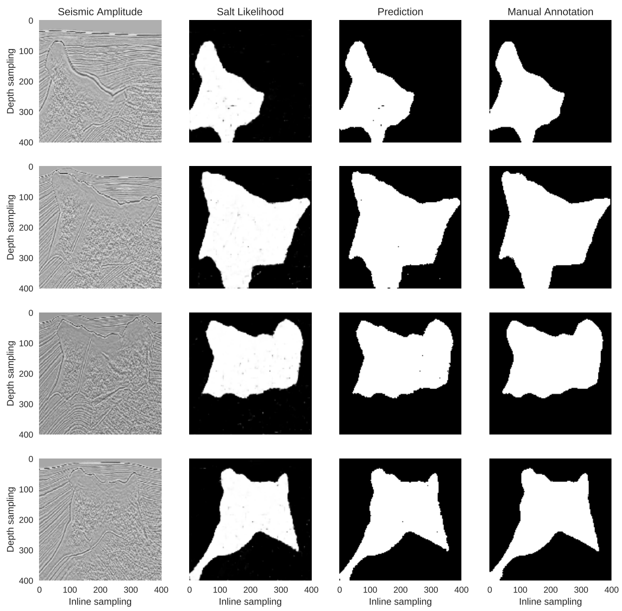

Figure 2: Selected training samples and their network output visualizations. The 4 rows represent 4 crossline samples extracted at inline locations: `[0, 150, 250, 350]`. From left to right, the first column show seismic amplitude images; the second column show probability outputs from softmax classifier of the network; the third column show salt detection prediction results generated by max-likelihood class; the fourth column show manual annotations used in the training.

VALIDATION TESTS

We first test the performance of the trained model at different crossline slices. Figure 3 shows the network output of these unseen crossline slices. Since these slices are still crossline slices, they share some similar features with the training data. It is noticeable that some noisy artifacts appear as "holes" in the detected salt body; however, the global shape of the salt body is extracted accurately, especially on the top boundary of the salt. To visualize the result, we extract the top salt locations with > 0.6 classification probability. The right column in Figure 3 clearly shows these top salt boundaries match seismic amplitudes accurately.

We then test the model on inline slices. The inline slices consists of images significantly different from the training set. The performance on this test can imply whether the network successfully learn important features independently to the view perspective. Figure 4 shows the network outputs of these inline slices. The first row of Figure 4 only contains a salt intrusion at the bottom-left corner, but the network seems to falsely classify some of the horizontal reflections as salt. The second to the seventh rows show that the salt bodies are correctly detected; however, the deeper parts of the images where seismic

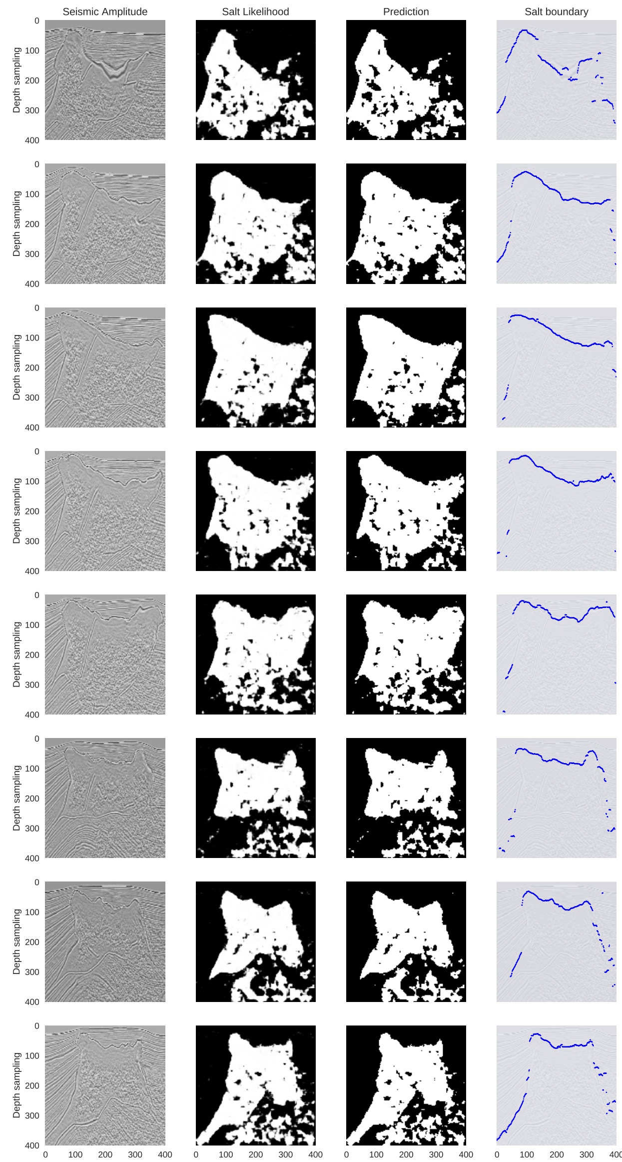

Figure 3: Selected crossline test samples and their network output visualizations. The 8 rows represent 8 crossline samples extracted at inline locations different from the ones used in training set: `[25, 75, 125, 175, 225, 275, 325, 375]`. From left to right, the first column show seismic amplitude images; the second column show probability outputs from softmax classifier of the network; the third column show salt detection prediction results generated by max-likelihood class; the fourth column show top salt boundaries by extracting the first occurence of salt likelihood > 0.6.

images are more noisy are incorrectly assigned to salt body. The eighth row shows that although deeper image part suffers from noise, the salt body in the shallow part is still correctly delineated. Except for the first row example, all examples show good detections of the top boundary of the salt body. Based on these results, we conclude that the proposed method can generalize well even when trained with only small dataset; the top boundary detection is the most robust prediction by the network.

DISCUSSION

In addition to an interpretation result, the confidence of the interpretation is also an important component in the decision making process. While conventional salt body classification methods lack uncertainty analysis, our proposed method can be extended for quantitative model uncertainty estimation.

Bayesian Segnet (Kendall et al., 2015) was developed to use Monte Carlo Dropout (Gal and Ghahramani, 2016) at test time to generate a posterior distribution of pixel class labels in the semantic segmentation. This model uncertainty is significantly different to the probabilities obtained from a softmax classifier as output from the traditional network. The softmax function approximates relative probabilities between the class labels, but not an overall measure of the model's uncertainty.

The model uncertainty can be used to infer the confidence of a salt image segmentation. Our future research will focus on deep learning based model uncertainty estimations for seismic interpretation.

CONCLUSIONS

We propose a method for an end-to-end automatic salt body detection in seismic image based on a deep convolutional network. The encoder-decoder architecture allows for extracting essential information from training data, and results in high accuracy.

We tested the model on the SEAM Phase 1 dataset. With limited amount of manually prepared training samples, the model successfully generalizes to unseen seismic slices, including both inline and crossline directions, and produces accurate salt body detection results compared with manual interpretation. We believe this method has a future potential for fast automated seismic interpretation with quantitative uncertainty analysis.

ACKNOWLEDGMENTS

We appreciate the financial support from sponsors of the Texas Consortium for Computational Seismology (TCCS). We thank NVIDIA GPU Grant Program for providing the Titan Xp.

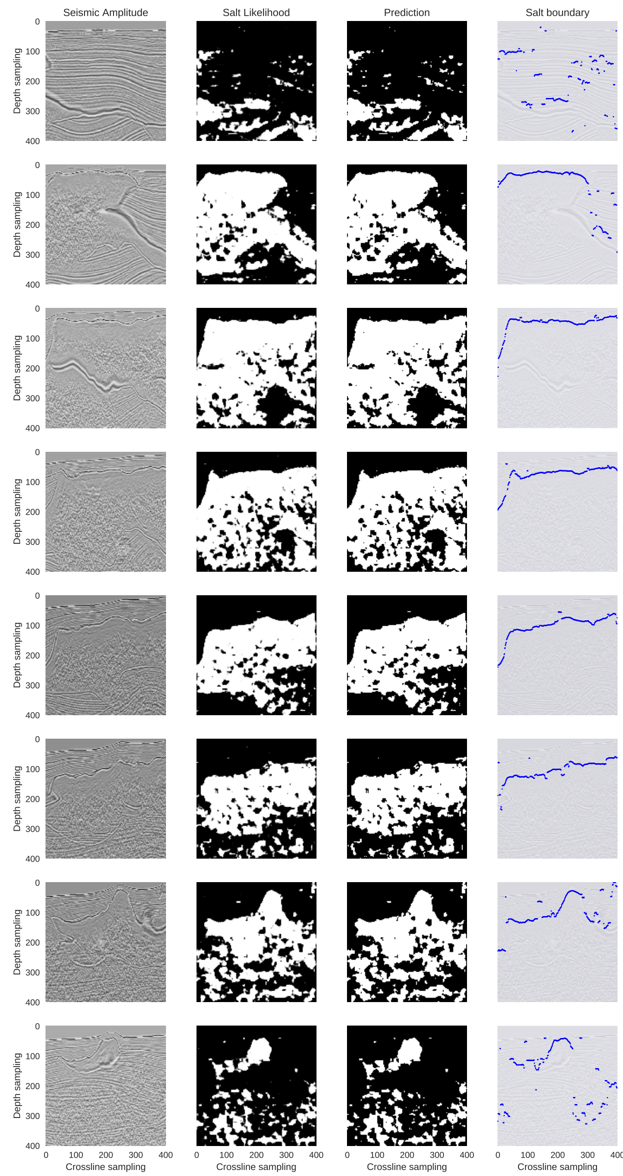

Figure 4: Selected inline test samples and their network output visualizations. The 8 rows represent 8 inline samples extracted at crossline locations: `[25, 75, 125, 175, 225, 275, 325, 375]`. Notice the difference in image contents compared to other inline images. From left to right, the first column show seismic amplitude images; the second column show probability outputs from softmax classifier of the network; the third column show salt detection prediction results generated by max-likelihood class; the fourth column show top salt boundaries by extracting the first occurence of salt likelihood > 0.6.

REFERENCES

Araya-Polo, M., T. Dahlke, C. Frogner, C. Zhang, T. Poggio, and D. Hohl, 2017, Automated fault detection without seismic processing: The Leading Edge, **36**, 208–214.

Asjad, A., and D. Mohamed, 2015, A new approach for salt dome detection using a 3D multidirectional edge detector: Applied Geophysics, **12**, 334–342, https://doi.org/10.1007/s11770-015-0512-2.

Badrinarayanan, V., A. Kendall, and R. Cipolla, 2017, SegNet: A deep convolutional encoder-decoder architecture for scene segmentation: IEEE Transactions on Pattern Analysis and Machine Intelligence, **39**, 2481–2495, https://doi.org/10.1109/tpami.2016.2644615.

Brostow, G. J., J. Shotton, J. Fauqueur, and R. Cipolla, 2008, Segmentation and recognition using structure from motion point clouds: European Conference on Computer Vision, Springer, 44–57.

Dahlke, T., M. Araya-Polo, C. Zhang, and C. Frogner, 2016, Predicting geological features in 3D seismic data: Presented at the Neural Information Processing Systems (NIPS).

Fehler, M. C., and P. J. Keliher, 2011, SEAM phase I: Challenges of subsalt imaging in tertiary basins, with emphasis on deepwater Gulf of Mexico: SEG.

Frogner, C., Z. Chiyuan, H. Mobahi, M. Araya-Polo, and T. A. Poggio, 2015, Learning with a Wasserstein loss: Presented at the Neural Information Processing Systems (NIPS).

Gal, Y., and Z. Ghahramani, 2016, Dropout as a Bayesian approximation: Representing model uncertainty in deep learning: International Conference on Machine Learning, 1050–1059.

Grangier, D., L. Bottou, and R. Collobert, 2009, Deep convolutional networks for scene parsing: Presented at the ICML 2009 Deep Learning Workshop.

Haukås, J., O. R. Ravndal, B. H. Fotland, A. Bounaim, and L. Sonneland, 2013, Automated salt body extraction from seismic data using the level set method: First Break, **31**, 35–42.

He, K., X. Zhang, S. Ren, and J. Sun, 2015, Delving deep into rectifiers: Surpassing human-level performance on imagenet classification: Proceedings of the IEEE International Conference on Computer Vision, 1026–1034.

Huang, L., X. Dong, and T. E. Clee, 2017, A scalable deep learning platform for identifying geologic features from seismic attributes: The Leading Edge, **36**, 249–256, https://doi.org/10.1190/tle36030249.1.

Hudec, M. R., M. P. Jackson, B. C. Vendeville, D. D. Schultz-Ela, and T. P. Dooley, 2011, The salt mine: A digital atlas of salt tectonics: Bureau of Economic Geology 5.

Ioffe, S., and C. Szegedy, 2015, Batch normalization. Accelerating deep network training by reducing internal covariate shift: International Conference on Machine Learning, 448–456.

Kendall, A., V. Badrinarayanan, and R. Cipolla, 2015, Bayesian segnet. Model uncertainty in deep convolutional encoder-decoder architectures for scene understanding: arXiv, abs/1511.02680.

Kingma, D. P., and J. Ba, 2014, Adam: A method for stochastic optimization: arXiv, abs/1412.6980.

Lomask, J., R. G. Clapp, and B. Biondi, 2007, Application of image segmentation to tracking 3D salt boundaries: Geophysics, **72**, no. 4, P47–P56, https://doi.org/10.1190/1.2732553.

Marfurt, K. J., and T. M. Alves, 2014, Pitfalls and limitations in seismic attribute interpretation of tectonic features: Interpretation, **3**, no. 1, SB5–SB15, https://doi.org/10.1190/int-2014-0122.1.

Odena, A., V. Dumoulin, and C. Olah, 2016, Deconvolution and checkerboard artifacts: Distill, **1**, e3.

Ramirez, C., G. Larrazabal, and G. Gonzalez, 2016, Salt body detection from seismic data via sparse representation: Geophysical Prospecting, **64**, 335–347.

Ronneberger, O., P. Fischer, and T. Brox, 2015, U-net. Convolutional networks for biomedical image segmentation: International Conference on Medical Image Computing and Computer-assisted Intervention, Springer, 234–241.

Ross, C. P., and D. M. Cole, 2017, A comparison of popular neural network facies-classification schemes: The Leading Edge, **36**, 340–349, https://doi.org/10.1190/tle36040340.1.

Sturgess, P., K. Alahari, L. Ladicky, and P. H. Torr, 2009, Combining appearance and structure from motion features for road scene understanding: Presented at the BMVC 2012-23rd British Machine Vision Conference.

Waldeland, A., and A. Solberg, 2017, Salt classification using deep learning: 79th Annual International Conference and Exhibition, EAGE, Extended Abstracts, https://doi.org/10.3997/2214-4609.201700918.

Wang, Z., T. Hegazy, Z. Long, and G. AlRegib, 2015, Noise-robust detection and tracking of salt domes in postmigrated volumes using texture, tensors, and subspace learning: Geophysics, **80**, no. 6, WD101–WD116, https://doi.org/10.1190/geo2015-0116.1.

Wu, X., 2016, Methods to compute salt likelihoods and extract salt boundaries from 3D seismic images: Geophysics, **81**, no. 6, IM119–IM126, https://doi.org/10.1190/geo2016-0250.1.

Wu, X., S. Fomel, and H. Michael, 2017, Fast salt boundary interpretation with optimal path picking: 87th Annual International Meeting, SEG, Expanded Abstracts, https://doi.org/10.1190/segam2017-17782682.1.

Zhang, C., C. Frogner, M. Araya-Polo, and D. Hohl, 2014, Machine-learning based automated fault detection in seismic traces: 76th Annual International Conference and Exhibition, EAGE, Extended Abstracts, https://doi.org/10.3997/2214-4609.20141500.

Zhao, T., 2017, Machine assisted quantitative seismic interpretation: Ph.D. thesis, University of Oklahoma.

10.1190/segam2018-2997304.1